

Arsenic removal from aqueous solutions by mixed magnetite–maghemite nanoparticles

Saidur Rahman Chowdhury · Ernest K. Yanful ·
Allen R. Pratt

Received: 21 March 2010 / Accepted: 8 November 2010
© Springer-Verlag 2010

Abstract In this study, magnetite–maghemite nanoparticles were used to treat arsenic-contaminated water. X-ray photoelectron spectroscopy (XPS) studies showed the presence of arsenic on the surface of magnetite–maghemite nanoparticles. Theoretical multiplet analysis of the magnetite–maghemite mixture ($\text{Fe}_3\text{O}_4\text{-}\gamma\text{Fe}_2\text{O}_3$) reported 30.8% of maghemite and 69.2% of magnetite. The results show that redox reaction occurred on magnetite–maghemite mixture surface when arsenic was introduced. The study showed that, apart from pH, the removal of arsenic from contaminated water also depends on contact time and initial concentration of arsenic. Equilibrium was achieved in 3 h in the case of 2 mg/L of As(V) and As(III) concentrations at pH 6.5. The results further suggest that arsenic adsorption involved the formation of weak arsenic–iron oxide complexes at the magnetite–maghemite surface. In groundwater, arsenic adsorption capacity of magnetite–maghemite nanoparticles at room temperature, calculated from the Langmuir isotherm, was 80 $\mu\text{mol/g}$ and Gibbs free energy (ΔG^0 , kJ/mol) for arsenic removal was

−35 kJ/mol, indicating the spontaneous nature of adsorption on magnetite–maghemite nanoparticles.

Keywords Arsenic · Groundwater · Magnetite–maghemite nanoparticles · Langmuir isotherm · Adsorption

Introduction

Elemental arsenic ranks twentieth in abundance in the earth's crust, fourteenth in seawater and twelfth in the human body (Shih 2005). Both organic and inorganic arsenic are found in natural waters, but organic arsenic is of less environmental concern as it undergoes biotransformation and detoxification through methylation. Inorganic arsenic in aquatic environment has different oxidation states. The oxidation states −3 and 0 are very rare whereas +3 and +5 are commonly found in water systems depending on the redox conditions. As(III) is found primarily as H_3AsO_3^0 , $\text{H}_2\text{AsO}_3^{3-}$, HAsO_3^{2-} , and AsO_3^{3-} under reducing environment whereas different hydrolyzed species of As(V), namely H_3AsO_4^0 , $\text{H}_2\text{AsO}_4^{-}$, HAsO_4^{2-} , and AsO_4^{3-} , exist in water under oxidizing environment (Anderson et al. 1976). Although environmental restrictions and regulations have controlled the production and use of arsenic and its compounds, they are still extensively used in metallurgy, agriculture, forestry, electronics, pharmaceuticals, glass, and the ceramic industry. Arsenic causes wide-spread groundwater contamination. Evidence of chronic arsenicosis has been observed in populations ingesting arsenic-contaminated drinking water in many parts of the world. Major sources of arsenic are geologic formations such as soil and bedrocks, weathering of rocks, mine tailings, industrial wastes discharge, fertilizers,

S. R. Chowdhury (✉)
Department of Civil and Environmental Engineering,
University of Western Ontario, Spencer Engineering Building,
London, ON N6A 5B9, Canada
e-mail: saidurc@yahoo.com

E. K. Yanful
Department of Civil and Environmental Engineering,
University of Western Ontario, London, ON N6A 5B9, Canada
e-mail: eyanful@eng.uwo.ca

A. R. Pratt
CANMET Mining and Mineral Sciences Laboratories,
Natural Resources Canada, Ottawa K1A 0G7, Canada
e-mail: Allen.Pratt@NRCan-RNCan.gc.ca

agricultural use of pesticides, smelting of metals, and burning of fossil fuels (Karim 2000; Neff 1997).

Several methods are used to remedy arsenic contamination. Those treatment methods are precipitation, electrochemical reduction, adsorption, ion exchange, solvent extraction, nano filtration, and reverse osmosis (Mayo et al. 2007; Hu et al. 2004). However, as recently noted by Hossain et al. (2005), these technologies do not perform well in actual field trials and improved systems are needed. As(III) adsorption on different sorbents such as coconut husk carbon, carbon from fly ash, iron-oxide-coated polymeric material, and hybrid polymeric sorbent has been investigated (Demarco et al. 2003; Ioannis and Anastasios 2002, and Manju et al. 2000). Iron and iron-coated sand, iron-coated activated carbon (Petrusevski et al. 2002), and granular ferric hydroxides (Driehaus and Jekel 1998) have also been used as adsorbents. However, their use is limited due to high operation cost, sludge formation, and technical difficulties in the preparation of materials. Naturally occurring ores and minerals, namely kaolinite (Guha and Chaudhuri 1990), magnetite (Yean et al. 2005; Shipley et al. 2009), maghemite (Lim et al. 2009), hematite, and feldspar (Prasad 1994), have also been used for the adsorption of arsenic though not as extensively as other materials.

Magnetite–maghemite ($\text{Fe}_3\text{O}_4-\gamma\text{-Fe}_2\text{O}_3$) nanoparticles are potential sorbents for arsenic removal in drinking water and are therefore suitable for treating arsenic-contaminated water. As maghemite and magnetite are generally found to be an oxidation product of iron, the association of the two minerals would be a common occurrence in nature (Grosvenor et al. 2004a). In this study, commercially prepared 20–40 nm ‘magnetite’ particles, identified in subsequent laboratory characterization to be mixed magnetite–maghemite, were used for the removal of arsenic from synthetic stock solution as well as from natural groundwater. Magnetite–maghemite mixture has affinity for heavy metals by adsorbing them from a liquid phase. To capitalize on this advantage of mixed magnetite–maghemite particles, the present study aimed to investigate the effectiveness of nano-size magnetite–maghemite particles in contaminated groundwater remediation. X-ray photoelectron spectroscopy (XPS) was employed to probe the interactions of the sorbent with arsenic. The overall purpose of the study was to investigate the performance of magnetite–maghemite nanoparticles in arsenic removal by examining the mechanism(s) of inorganic arsenic uptake. This is one of the very few studies that have, to date, examined arsenic removal from stock solution as well as from natural groundwater by mixed magnetite–maghemite nanoparticles. Although magnetite and maghemite may separately remove greater amounts of arsenic from solution than the mixture (Shipley et al. 2009; Lim et al. 2009), it is

probably more realistic and practical to examine the removal efficiency of the mixture because of the common association of the two minerals in nature. In addition, most commercial grade ‘magnetite’ nanoparticles used in field scale remediation of arsenic contamination would likely be a mixture of magnetite and maghemite because of slight oxidation during storage or shipping.

Materials and methods

Sample preparation

All solutions used in the experiments were prepared from certified reagent-grade chemicals, which were used without further purification. Solutions were prepared with de-ionized water. Glass volumetric flasks and reaction vessels were treated with 10% HNO_3 and rinsed several times with de-ionized water before they were used. Both As(V) and As(III) stock solutions were prepared by dissolving arsenic oxides (As_2O_5 and As_2O_3) powder in de-ionized water, using 4 g/L NaOH since both oxides have enhanced solubility in NaOH solution. For each stock solution, redox potential was measured using a WTW Multi 340i ORP electrode (Wellheim, Germany) to confirm the targeted As(V) and As(III).

Commercially available 20–40 nm ‘magnetite’ particles were obtained from Reade Advanced Materials (Rhode Island, U.S.A.). Subsequent laboratory characterization prior to the adsorption studies, presented later in this paper, indicated that the particles were actually a mixture of magnetite and maghemite. The BET surface area of the mixed particles provided by the manufacturer was $60 \text{ m}^2/\text{g}$. The mixture arrived in powder form in an airtight plastic bag. Further examination of the as-received sample showed that the particles were dispersed and of a purity of more than 98%. Impurities were identified through subsequent laboratory characterization. The particles had black and spherical morphology, and the bulk density was measured to be 0.84 g/cm^3 . Figure 1 shows $200,000\times$ magnification image of magnetite–maghemite nanoparticles (20–40 nm) using Hitachi S4500 scanning electron microscopy (SEM). A $200,000\times$ magnification was also used to check surface porosity, but the image did not show the presence of pores at $200,000\times$ magnification and the mixture of magnetite–maghemite appeared to be highly uniform.

Arsenic-contaminated groundwater collected from shallow aquifers in Bangladesh was also used in the study. All samples were immediately acidified with 2% HNO_3 upon collection in the field to prevent the precipitation of Fe-As compound and were kept in plastic bottles. The samples were collected from Srinagar, Munshiganj, and Sylhet Golapganj in Bangladesh. Groundwater samples

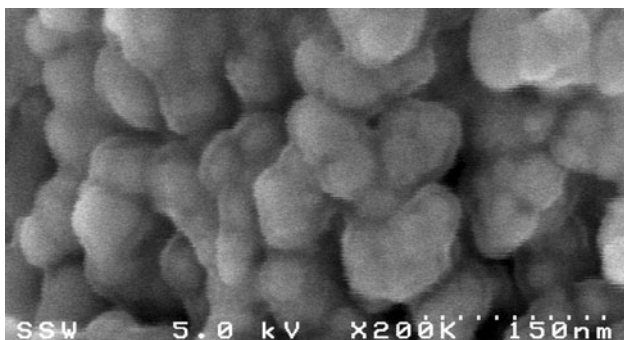


Fig. 1 200,000 \times magnification image of magnetite–maghemite nanoparticles (20–40 nm) using Hitachi S4500 scanning electron microscopy (SEM)

were spiked to check the quality of the analytical methods. Known concentrations of arsenic stock solution were added to desired amount of groundwater to increase the initial concentration of arsenic. Different initial concentrations of arsenic in groundwater samples were prepared to investigate the adsorption capacity of 20–40 nm magnetite–maghemite particles in the removal of arsenic from contaminated groundwater.

Adsorption experiments

Batch experiments were run for complete adsorption on the magnetite–maghemite mixture. The mixture was dispersed in solution in a sonication bath for 20 min. Known amount of arsenic stock solution was mixed with magnetite–maghemite mixture solution and held in a slowly rotating rack of a shaker that provided a gentle end-over-end tumbling (28 rpm) for 24 h. After shaking, the mixtures were centrifuged at 5,000 rpm for 30 min. The supernatant solutions were separated, and solid samples were dried in a vacuum desiccator. Then dried arsenic adsorbed magnetite–maghemite nanoparticles were kept in an airtight ceramic dish to prevent any reaction with air. The supernatant solutions were filtered through 0.2 μm Nalgene Surfactant-Free Cellulose Acetate (SFCA) syringe filters (VWR International, Mississauga, ON, Canada). The pH of each solution was measured immediately after sampling for As measurements. The filtrate was acidified with 1% nitric acid. ICP-AES (inductively coupled plasma-atomic emission spectroscopy) was used to measure arsenic concentrations in the filtrate. The minimum detection limit of ICP-AES for arsenic is 0.01 mg/L.

Equilibrium modeling

The experimental data obtained at pH 5 were applied to the linearized forms of Langmuir and Freundlich (Eqs. 1, 2, respectively), which were suitable for measuring

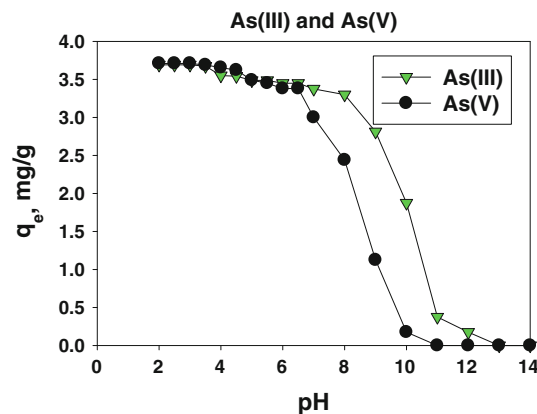


Fig. 2 Effect of pH on the adsorption of As(III) and As(V) by magnetite–maghemite

adsorption as well as to interpret the nature of adsorption of arsenic on magnetite–maghemite nanoparticles.

$$C_e/q_e = 1/bq_m + C_e/q_m \quad (1)$$

$$\ln q_e = \ln K + (1/n * \ln C_e) \quad (2)$$

where C_e and q_e are equilibrium solute concentration (mg/L) and equilibrium adsorption capacity (mg/g), respectively. The other parameters, q_m , b , and n are isotherm constants. The value of q_m is adsorption maxima or adsorption capacity (mg/g) in Eq. 1.

Instrumentation for XPS

A Kratos Axis Ultra XPS instrument was used to measure all spectra. All samples were analyzed with a monochromatic A $K\alpha$ X-ray source using analysis chamber pressures of 10^{-7} – 10^{-6} Pa. The resolution function of the instrument was found to be 0.35 eV using the silver Fermi edge (Grosvenor et al. 2004b). The charge neutralizer filament was used during all experiments to control charging of the samples. The conditions applied for the survey scans were

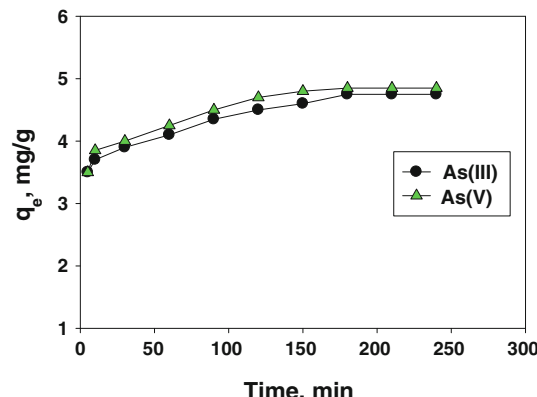
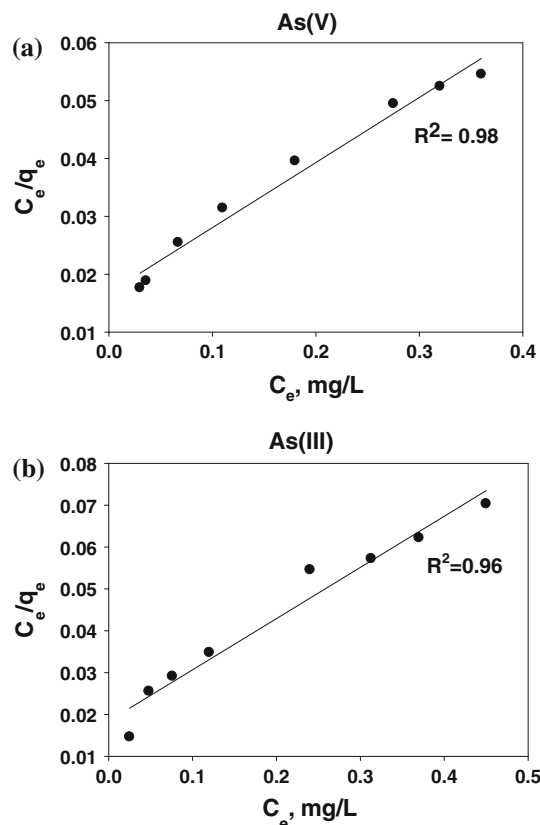


Fig. 3 Effect of contact time on the adsorption of As(III) and As(V) by magnetite–maghemite at pH 6.5

Table 1 Comparison of adsorption isotherms for As(III) and As(V) adsorption by magnetite–maghemite nanoparticles at room temperature

Arsenic species pH	Correlation coefficient for different isotherms, R^2	
	Langmuir	Freundlich
As(III) 5	0.96	0.97
As(V) 5	0.98	0.98

**Fig. 4** Langmuir isotherm plots for As(III) and As(V) adsorption by magnetite–maghemite nanoparticles (initial concentration 0.7–3 mg/L; contact time 24 h; pH = 5; magnetite–maghemite nanoparticles dosage 0.4 g/L)

as follows: energy range = 1100–0 eV, pass energy = 160 eV, step size = 0.7 eV, sweep time = 180 s and X-ray spot size = $700 \times 400 \mu\text{m}$. An energy range of 40–20 eV was used for the high-resolution spectra, depending on the peak being examined, with a pass energy of 10 eV and a step size of 0.05 eV.

Results and discussion

Effect of pH

The effect of pH on As(III) and As(V) adsorption by magnetite–maghemite nanoparticles was studied in the pH

Table 2 Calculated values of the dimensionless separation factor “r” for As(V) and As(III) adsorption by magnetite–maghemite nanoparticles at 22°C

Metals	C_o (mg/L)	b (L/mg)	r	$-\Delta G^0$ (kJ mol $^{-1}$)
As(V)	0.71 (min)	6.7	0.173	32.6
As(V)	3 (max)	6.7	0.05	32.6
As(III)	0.71 (min)	6.63	0.175	32.5
As(III)	3 (max)	6.63	0.05	32.5

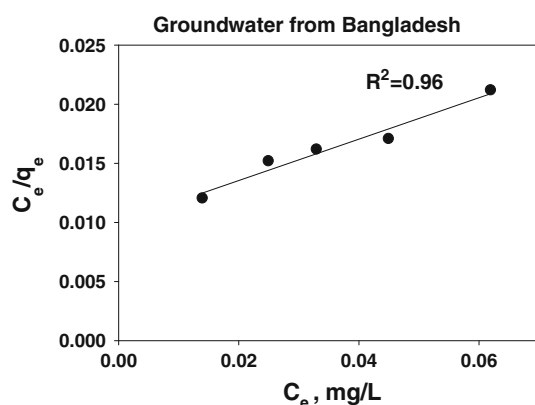
range of 1–14 at the contact time of 24 h and As(III) and As(V) concentrations of 1.5 mg/L each. Figure 2 illustrates the effect of pH on adsorption density (q) in mg/g which is a measure of the degree of adsorption. The data show that adsorption decreases as pH increases. Variations in As(V) adsorption on magnetite–maghemite in the pH range 2–6.5 were found to be small. As(V) adsorption decreased sharply above pH 7. Again, variations in As(III) adsorption on magnetite–maghemite in the pH range 2–9 were negligible. The adsorbed amount of arsenic species was 3.69 mg/g for As(III) and 3.71 mg/g for As(V) at pH 2. These results clearly show that magnetite–maghemite nanoparticles can adsorb As(III) and As(V) more readily in an acidic pH range.

The surface hydroxyl groups, arising from adsorption of water or from structural OH, are the functional groups of iron oxides. They contain a double pair of electrons together with a dissociable hydrogen atom which can help them to react with both acids and bases. Charge on the iron oxide surface is established by the dissociation (ionization) of the surface hydroxyl groups. This situation corresponds to adsorption or desorption of protons depending on the pH of the solution. According to Cornell and Schwertmann (1996), magnetite generates Fe^{2+} and its hydrolysis products (FeOH^+ , $\text{Fe}(\text{OH})_2^0$, and $\text{Fe}(\text{OH})_3^-$) depending on the solution pH. According to Cornell and Schwertmann (1996), acidity constant of magnetite (69.2% of used adsorbent), pK_{a1} is 5.6. Thus, at $\text{pH} < 5.6$, dominant functional groups of iron oxide surface would be Fe^{2+} or FeOH^+ . Thus, iron oxide would attract negative arsenic species at low pH. At higher pH, the surface hydroxyl groups on the iron oxide surface are $\text{Fe}(\text{OH})_2^0$, and $\text{Fe}(\text{OH})_3^-$. Thus, in this study, negative charge iron oxide surface repelled negative charge arsenic species at the higher pH value. Maghemite is formed through the oxidation of magnetite; therefore, $\text{Fe}(\text{III})$ in solution would form hydrated ferric oxides (HFO) nanoparticles. Even if As(V) is reduced to As(III), adsorption will keep arsenic on the magnetite–maghemite surface through a Lewis acid base (LAB) interactions.

The variation in removal efficiency at different pH values may be attributed to the affinities of the mixed magnetite–maghemite for the different species of As(V)

Table 3 Groundwater sample chemistry after acidification

Parameters	Concentration present		
	Sample ID DR-18	Sample ID DR-34	Sample ID Sylhet
Total Arsenic ($\mu\text{g/L}$)	301	443	53.7
pH	1.8	2	5
Electrical conductivity (EC) ($\mu\text{S/cm}$)	21,800 at 17°C	20,500 at 17°C	178 at 17°C
Chloride (Cl^-) (mg/L)	12.51	14.85	180
Nitrate (NO_3^- -N) (mg/L)	3,900	3,500	1.35
Phosphate (PO_4^{3-}) (mg/L)	0.89	3.63	0.6
Sulfate (SO_4^{2-}) (mg/L)	<1.0	<1.0	<0.5
Redox potential (mV)	+595	+629	+350

**Fig. 5** Langmuir isotherm plot for arsenic adsorption from natural groundwater by magnetite-maghemite nanoparticles (initial concn. 0.285–1.4 mg/L; contact time 24 h; pH 2; magnetite-maghemite nanoparticles dosage 0.4 g/L)

and As(III) present at different pH values, namely AsO_4^{3-} , HAsO_4^{2-} , H_2AsO_4^- , H_3AsO_4 , AsO_3^{3-} , HAsO_3^{2-} , H_2AsO_3^- , and H_3AsO_3^0 . At pH 2.3–6.9, the predominant species of As(V) is H_2AsO_4^- (Nordstrom and Archer 2003). The adsorption free energy of H_2AsO_4^- ion may be lower than that of HAsO_4^{2-} and AsO_4^{3-} , and this would explain why H_2AsO_4^- is more favorably adsorbed than HAsO_4^{2-} and AsO_4^{3-} . From literature, the first pKa value for As(III) in aqueous solution is 9.17 (Nordstrom and Archer 2003) and the predominant species of As(III) at pH below 9.17 is neutral or chargeless, namely H_3AsO_3^0 . Thus, the adsorption of the nonionic form of As(III) on magnetite-maghemite surface would not change significantly at pH below 9.17. However, at increasing pH values (beyond 9.17), As(III) uptake decreases slowly because of the higher concentration of OH^- ion present in the reaction mixtures.

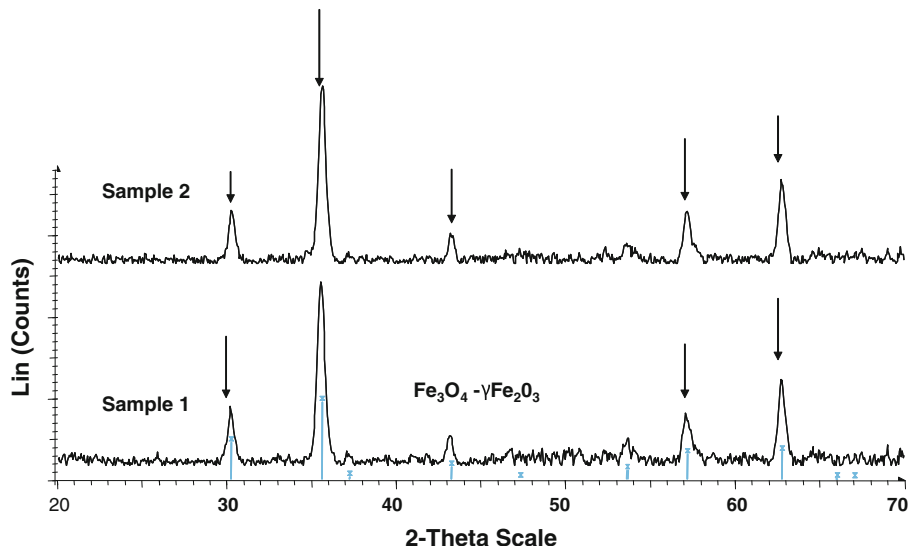
Yean et al. (2005) showed from potentiometric titrations that the surface of magnetite particles had a positive surface charge up to pH 6.8, a point of zero charge of 6.8, and a negative surface charge in the pH range 6.8–9.5. According to Tuutijärvi et al. (2009), maghemite has a point of zero charge at pH_{pzc} 7.5 and the more acidic the

condition the more positive was the surface charge of the adsorbent and, accordingly, the more attractive to negative As species. Thus, magnetite-maghemite particles can adsorb either negatively or positively charged species by electrostatic attraction depending on pH.

Equilibrium time determination

The kinetics of As(V) and As(III) adsorption were studied by varying the contact time between magnetite-maghemite and the respective solution from 10 to 240 min using 0.4 g/L adsorbent at a metalloid (As) concentration of 2 mg/L and pH 6.5. The adsorption of As(V) and As(III) on magnetite-maghemite nanoparticles at fixed metal concentration is shown in Fig. 3. The adsorption on mixed magnetite-maghemite seems to take place in two phases. The first phase involved rapid metalloid adsorption within 10 min of contact time because of the availability of the adsorption sites in the solution and was followed by subsequent slower uptake. In addition, the rapid metalloid uptake by magnetite-maghemite nanoparticles is perhaps attributed to external surface adsorption, which is different from the microporous adsorption process. Since nearly all the sorption sites of mixed magnetite-maghemite nanoparticles exist in the exterior of the adsorbent compared with the porous adsorbent, it is easy for arsenic species to access these active sites, thus resulting in a rapid approach to equilibrium. For 2 mg/L of As(V) and As(III) concentrations, equilibrium was achieved in 3 h when experiments were run at pH 6.5. At equilibrium, adsorbed amount of arsenic As(V) and As(III) was almost 4.85 and 4.75 mg/g, respectively, representing 92% of As(V) and 91% of As(III) removal efficiencies by magnetite-maghemite nanoparticles. In addition, the adsorption of As(III) and As(V) on the mixed magnetite and maghemite mixture may involve two steps. First, As(III) and As(V) species migrate from the bulk fluid phase to the outer particle surface of the adsorbent for contact (film diffusion). Second, there might be electro-static attraction or reaction occurring between adsorbate (As(III) or As(V) species) and adsorbent.

Fig. 6 XRD patterns showing magnetite–maghemite particles: sample 1 before arsenic adsorption; sample 2 after arsenic adsorption



Adsorption isotherms

The adsorption data were fitted with the isotherm equations to identify the most appropriate adsorption parameters for future modeling and scale up. Calculated correlation coefficients for the isotherms using linear regression analysis for As(III) and As(V) adsorption at pH 5 are shown in Table 1. As indicated, the results show that adsorption by magnetite–maghemite nanoparticles is well described by the Freundlich and Langmuir isotherm equations. The Langmuir isotherm model can be used to determine adsorption maxima, q_m (mg/g). Figure 4 shows Langmuir plots for As(III) and As(V) adsorption by magnetite–maghemite nanoparticles. Gupta and Chen (1978) noted that Langmuir adsorption is a reversible phenomenon and that the coverage is monolayer.

A number of researchers have observed that several adsorption processes follow the Langmuir isotherm. Examples include As(III) adsorption by hematite (Singh et al. 1988), As(III) and As(V) adsorption by magnetite (Shipley et al. 2009), activated carbon, activated bauxite and activated alumina (Gupta and Chen 1978) and amorphous iron hydroxide (Harper and Kingham 1992), and As(V) adsorption by amorphous aluminum hydroxide (Anderson et al. 1976). Previous studies have presented maximum As(III) adsorption capacity for hematite, activated bauxite, activated alumina, iron(III) hydroxide loaded coral limestone (Fe-coral), and magnetite are 2.63, 16, 14, 0.17 μmol/g and 0.2 mmol/g, respectively (Gupta and Chen 1978; Singh et al. 1988; Harper and Kingham 1992; Maeda et al. 1992; Ohe et al. 2005). For As(V) adsorption by activated bauxite, activated alumina, activated carbon, Fe-coral and magnetite, the calculated maximum adsorption capacities are 52, 67, 10, 0.2 μmol/g, and 0.2 mmol/g (Gupta and Chen 1978; Maeda et al., 1992; Ohe et al.

2005), respectively. In the present study, As(III) and As(V) adsorption capacities of magnetite–maghemite nanoparticles at room temperature and pH 5, calculated from Langmuir isotherm, are 109 and 120 μmol/g. It is evident that magnetite–maghemite nanoparticles are more effective adsorbents than hematite and Fe-coral but less than magnetite.

Raven et al. (1998) reported that the maximum adsorption of As(V) on hydrated ferrous oxide (HFO) was approximately 0.25 mol As/mol Fe at pH 4.6 and 8.0. Dixit and Hering (2003) reported similar maximum sorption capacities for As(III) and As(V) on goethite, which was 16 mmol As/mol Fe. In the present study, As(V) and As(III) sorption maxima on 20–40 nm magnetite–maghemite particles was found to be 10 mmol As/mol Fe at pH 5. Despite the reported higher arsenic species removal from water by HFO and goethite, the findings on arsenic removal by magnetite–maghemite nanoparticles are still significant because magnetite–maghemite particles are found more in natural soil than HFO and goethite (Wang et al. 2008).

In order to calculate the adsorption efficiency of the process, the dimensionless equilibrium parameter was determined from the following equation:

$$r = 1/(1 + bC_0) \quad (3)$$

where r is a dimensionless separation factor, C_0 is the initial As(III) or As(V) concentration (mg/L) and b is the Langmuir isotherm constant (L/mg). A value of $r < 1$ represents favorable adsorption and a value greater than one represents unfavorable adsorption (Mckay et al. 1985). In this study, calculated values of r for all initial concentrations of As(III) and As(V) were found to be < 0.2 at room temperature (22°C). Thus, as shown in Table 2, it can be concluded that the adsorption of As(III) and As(V) on magnetite–maghemite nanoparticles was highly favorable

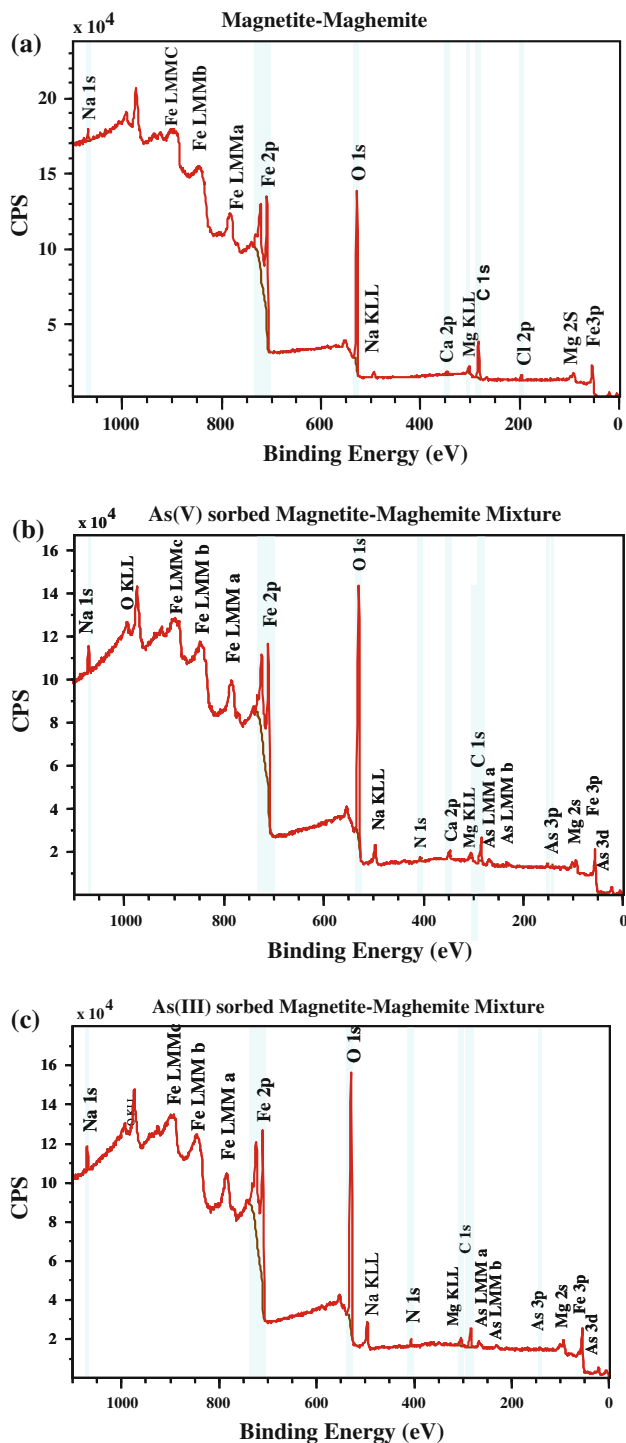


Fig. 7 XPS wide scan spectra of the **a** fresh magnetite–maghemite mixture **b** As(V) loaded magnetite–maghemite mixture **c** As(III) loaded magnetite–maghemite mixture

at the concentrations and temperature studied. Table 2 shows ‘*r*’ values of As(V) and As(III) at pH 5.

Standard Gibbs free energy (ΔG^0 , kJ/mol) for the adsorption process was calculated using the following equation:

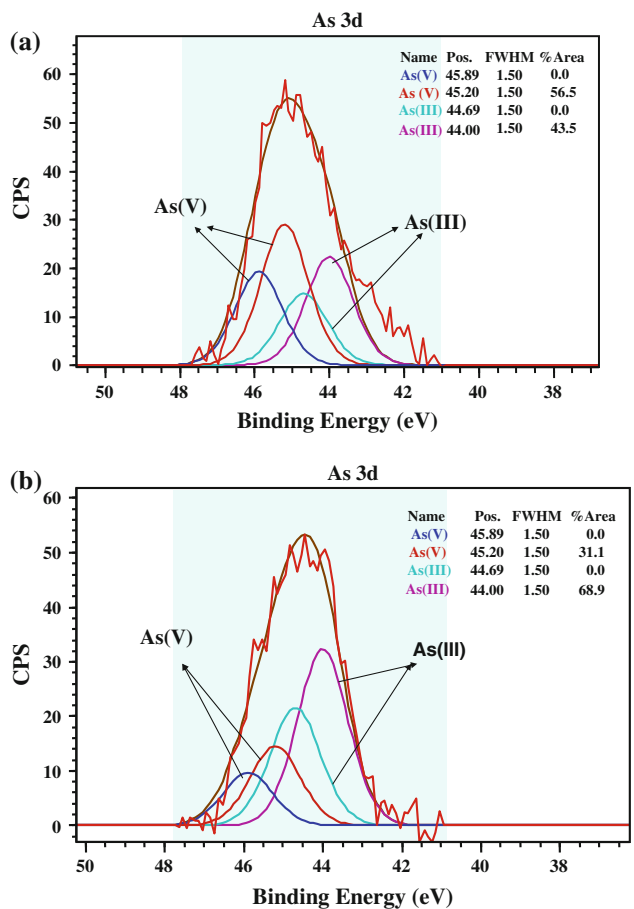


Fig. 8 As 3d XPS spectra of **a** As(V) loaded **b** As(III) loaded magnetite–maghemite mixture. (background subtracted in data)

$$\ln(1/b) = \Delta G^0 / RT \quad (4)$$

where *b* is the Langmuir constant related to the energy of adsorption, *R* is the ideal gas constant (8.314 J/K mol), and *T* is temperature (K). A negative ΔG^0 value indicates the reaction or process is spontaneous and thermodynamically stable, while a positive value suggests that the reaction or process is in the reverse direction. In this study, the negative ΔG^0 values obtained for As(III) and As(V) adsorption on magnetite–maghemite nanoparticles (Table 2) confirm the feasibility of the adsorption process and the spontaneous nature of adsorption.

Arsenic removal from groundwater

Groundwater collected from three wells in Bangladesh aquifers was found to contain relatively high concentrations of arsenic (>0.05 mg/L). The present study therefore examined the removal of the arsenic from groundwater using magnetite–maghemite nanoparticles as adsorbent. To prevent metal precipitation, the samples were acidified after collection. Table 3 shows groundwater sample

Table 4 Binding energies and relative content of As, C and O in adsorbents

Valence state	Sample	Elemental oxidation state	Binding energy (eV)	Peak area (%)	FWHM
As 3d	As(III) loaded sorbent	As(III) (As_2O_3)	44.69	0	1.5
		As(III) (As_2O_3)	44.0	68.9	1.5
		As(V) (As_2O_5)	45.89	0	1.5
		As(V) (As_2O_5)	45.2	31.1	1.5
As 3d	As(V) loaded sorbent	As(III) species (As_2O_3)	44.69	0	1.5
		As(III) (As_2O_3)	44.0	43.5	1.5
		As(V) (As_2O_5)	45.89	0	1.5
		As(V) (As_2O_5)	45.2	56.5	1.5
C 1s	Fresh magnetite–maghemite sorbent	O=C=O	288.87	6.1	0.98
		C–OH, C–O–C	286.30	13.9	1.31
		C=C, C–H	284.8	80.1	1.31
C 1s	As (III) loaded sorbent	O=C=O	288.62	12.7	1.38
		C–OH, C–O–C	286.30	12.6	1.39
		C=C, C–H	284.8	74.7	1.39
C 1s	As (V) loaded sorbent	O=C=O	288.35	12.6	1.9
		C–OH, C–O–C	286.30	10	1.5
		C=C, C–H	284.8	57.4	1.5
O 1s	Fresh magnetite–maghemite sorbent	Metal oxide (Fe–O)	529.86	70.7	1.13
O 1s	As (III) loaded sorbent	Metal oxide	530.03	75.2	1.32
O 1s	As (V) loaded sorbent	Metal oxide	529.83	74.5	1.74

chemistry after acidification. The redox potentials of the three samples after acidification were measured to be +595 mV, +629 mV at pH 2 and +350 mV at pH 5, indicating the presence of As(V) species (oxidation state +5) in each solution. Groundwater samples were also spiked with arsenic.

Arsenic contamination in groundwater of Bengal delta including Bangladesh has been observed not only as the severest natural disaster of the world but also as a threat to the social base of public society, as a new social tragedy, where more than 100 million people in 61 districts out of 64 are at the risk of severe arsenic hazard. Arsenic concentrations generally range from 0.25 µg/L to more than 1.6 mg/L (BGS 2001). To investigate the ability of magnetite–maghemite nanoparticles to remove these levels of arsenic from Bangladesh groundwater, samples were spiked to those concentration ranges. At the same time, some groundwater samples were kept at their natural arsenic concentrations. Thus, spiked groundwater samples containing different initial concentrations of arsenic were added to 20–40 nm magnetite in batch experiments to assess arsenic removal. Figure 5 shows arsenic adsorption on 20–40 nm magnetite–maghemite nanoparticles using 0.4 g/L adsorbent concentration and at pH 2 fitted to the Langmuir isotherm. As indicated, the Langmuir isotherm provides a reasonable fit to the experimental data, indicating favorable adsorption (Fig. 5). Arsenic adsorption capacity of magnetite–maghemite nanoparticles at room

temperature calculated from the Langmuir isotherm was 0.08 mmol/g. Gibbs free energy (ΔG^0 , kJ/mol) for arsenic removal from groundwater was –35 kJ/mol, indicating the spontaneous nature of adsorption on magnetite–maghemite nanoparticles.

X-ray photoelectron spectroscopy (XPS) analysis

The As-loaded magnetite–maghemite particles after As adsorption at fixed pH were characterized using XRD (X-ray diffraction) and XPS (X-ray photoelectron spectroscopy) techniques. The results from XRD analysis (Fig. 6) show that the identical peaks of the As-adsorbed particles match well with standard Fe_3O_4 – γ - Fe_2O_3 without other crystalline phases appearing after adsorption.

The elemental composition and chemical oxidation states of surface and near-surface species were investigated using XPS. All spectra were drawn and analyzed using the Casa-XPS software (Fairley 1999–2003). XPS wide scan spectra of fresh magnetite–maghemite and arsenic adsorbed magnetite–maghemite sorbents are illustrated in Fig. 7. Three major peaks at binding energies of 282.25, 348.05, 527.25, and 301.85 eV, designated for the C 1 s, Ca 2p, O1 s, and Mg KLL, respectively, are observed for the virgin sorbent (Fig. 7a). Significant changes can be found in Fig. 7b, c after As(III) and As(V) adsorption; the peak at binding energy of 348.05 eV for Ca 2p disappears in As(III) loaded sorbent while a new weak peak at binding

energy of about 45–46.7 eV for As 3d appears in arsenic sorbed magnetite–maghemite sorbents.

The As 3d spectrum of the arsenic adsorbed sorbent can be deconvoluted into two individual component peaks, which originate from the different valent arsenic atom and overlap on each other. According to Nesbitt and Pratt (1995) and Lim et al. (2009), the As 3d5/2 peak for As(III) and As(V) were set to binding energy ranges of 44.0 eV to 45.5 eV and 45.2 eV to 46.8 eV, respectively. As shown in Fig. 8, the peaks at binding energies of 44.5 and 45.2 eV can be assigned to the arsenite (As(III)) and arsenate (As(V)) atom, respectively. These two assignments reflect the different chemical valence of inorganic arsenic on the sorbent. The quantitative analysis of As(V) adsorbed sorbent obtained from Fig. 8a that 56.5% of As(V) and 43.5% of As(III) are present as demonstrated in Table 4. This result suggests the reduction of As(V) to As(III) on the sorbent surface. In Fig. 8b, the quantitative analysis of As(III) adsorbed sorbent shows 68.9% of As(III) and 29% of As(V) species on the sorbent surface. This result indicates solid-state oxidation–reduction between arsenate and arsenite on the surface of the sorbent. From Table 4 and according to Nesbitt and Pratt (1995), an As(III)-O bonded compound is found at 44.5 eV in the XPS spectra and it is clear that some amount of As(III) was oxidized to As(V) in As(III) loaded sorbent because of oxidation occurring during sample preparation.

The Fe 2p high-resolution spectra were fitted following the example of Pratt et al. (1994) using theoretical multiplet peak (Gupta and Sen 1974, 1975). The peak full width at half maximum (FWHM) was generally held to be between 1.0 and 1.5 eV. The XPS results, shown in Fig. 9, present the theoretical multiplet peaks for iron and arsenic adsorbed iron at the surface of the Fe_3O_4 and $\gamma\text{-Fe}_2\text{O}_3$ mixture. Theoretical multiplet analysis of the Fe_3O_4 – $\gamma\text{-Fe}_2\text{O}_3$ mixture gave 30.8% of maghemite and 69.2% of magnetite (Fig. 9a). After arsenic adsorption on the magnetite–maghemite mixture, it was found that the percent of maghemite increased to 47.2% (Fig. 9b) for As(V) adsorption and 70.5% (Fig. 9c) for As(III) adsorption. At the same time, the percentage of magnetite was reduced for both cases. Thus, the results show that a redox reaction occurred on the magnetite–maghemite mixture surface when arsenic was introduced. Changes in the relative abundance of Fe(II) and Fe(III) in magnetite and maghemite spectra (Fig. 9b, c) upon arsenite and arsenate sorption process are quantitatively elucidated as indicated in Table 4. It shows that the relative content of the Fe(II) decreases from 25.9 to 20.1% for As(V) loaded magnetite–maghemite sorbent indicating oxidation on mixed surface as well as increase in maghemite from 30.1 to 47.2%. The relative content of the Fe(II) decreased from 25.9 to 11.2% for As(III) loaded magnetite–maghemite sorbent resulting

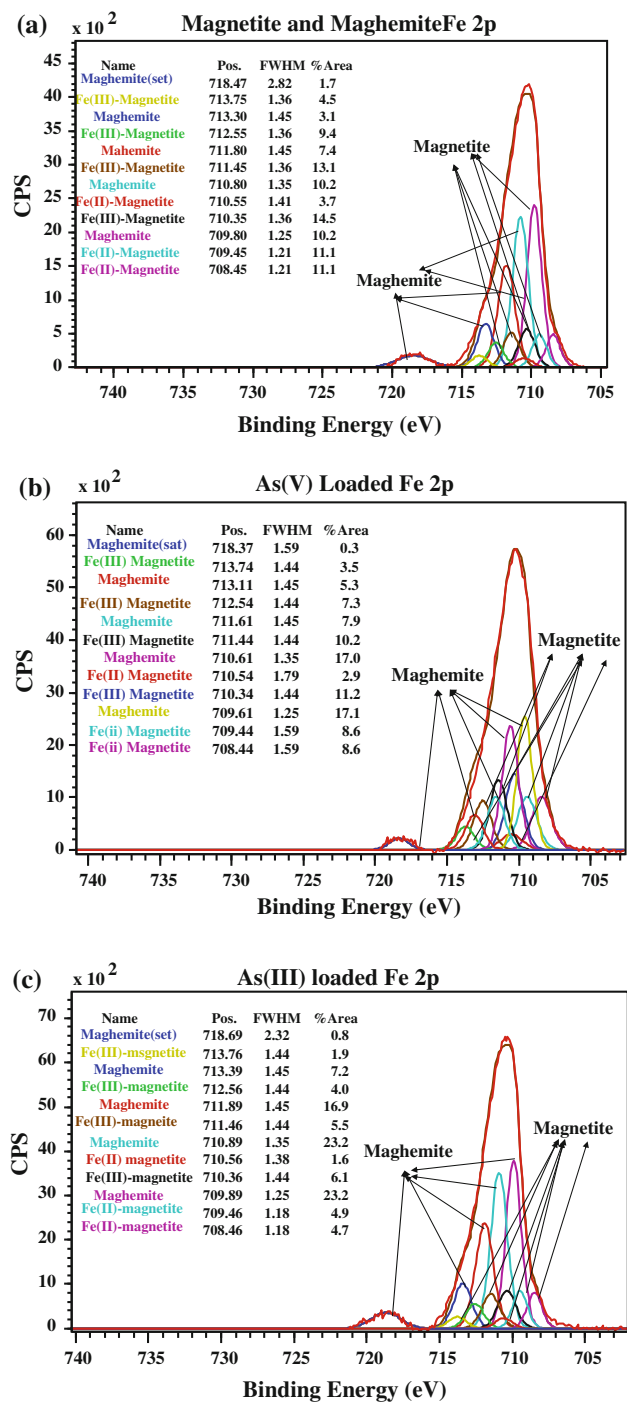


Fig. 9 XPS spectra **a** nanoscale magnetite–maghemite particles **b** As(V)-adsorbed magnetite–maghemite mixture particles at pH 5 **c** As(III)- adsorbed magnetite–maghemite mixture particles at pH 5

in the percent of maghemite increasing to 70.5% for As(III) adsorption. Again, smaller amount (41.5 to 32.2%) of Fe(III) decreases on As(V) loaded magnetite–maghemite sorbent in magnetite spectra (Fig. 9b) indicating decrease in magnetite content (69.1 to 52%) on mixed magnetite–maghemite sorbent. Table 5.

Table 5 Multiplet peak positions, FWHM and areas used to fit the XPS data

Sample name	Metal oxide	Binding energy (eV)	FWHM	Area (%)
Magnetite–maghemite mixture	Maghemite (sat)	718.37	1.59	0.3%
	Maghemite	713.30	1.45	3.1
	Maghemite	711.80	1.45	7.4
	Maghemite	710.80	1.35	10.2
	Maghemite	709.80	1.25	10.2
	Fe(III) Magnetite	713.75	1.36	4.5
	Fe(III) Magnetite	712.55	1.36	9.4
	Fe(III) Magnetite	711.45	1.36	13.1
	Fe(III) Magnetite	710.35	1.36	14.5
	Fe(II) Magnetite	710.55	1.41	3.7
As(V) loaded sorbent	Fe(II) Magnetite	709.45	1.21	11.1
	Fe(II) Magnetite	708.45	1.21	11.1
	Maghemite (sat)	718.37	1.59	0.3
	Maghemite	713.11	1.45	5.3
	Maghemite	711.61	1.45	7.9
	Maghemite	710.61	1.35	17.0
	Maghemite	709.61	1.25	17.1
	Fe(III) Magnetite	713.74	1.44	3.5
	Fe(III) Magnetite	712.54	1.44	7.3
	Fe(III) Magnetite	711.44	1.44	10.2
As(III) loaded sorbent	Fe(III) Magnetite	710.34	1.44	11.2
	Fe(II) Magnetite	710.54	1.79	2.9
	Fe(II) Magnetite	709.44	1.59	8.6
	Fe(II) Magnetite	708.44	1.59	8.6
	Maghemite (sat)	718.69	2.32	0.8
	Maghemite	713.39	1.45	7.2
	Maghemite	711.89	1.45	16.9
	Maghemite	710.89	1.35	23.2
	Maghemite	709.89	1.25	23.2
	Fe(III) Magnetite	713.39	1.45	7.2
Peak parameters were obtained from Grosvenor et al. (2004a, b)	Fe(III) Magnetite	712.56	1.44	4.0
	Fe(III) Magnetite	711.46	1.44	5.5
	Fe(III) Magnetite	710.36	1.44	6.1
	Fe(II) Magnetite	710.56	1.38	1.6
	Fe(II) Magnetite	709.46	1.18	4.9
	Fe(II) Magnetite	708.46	1.18	4.7

Peak parameters were obtained from Grosvenor et al. (2004a, b)

In XPS data, adventitious elements (carbon and oxygen) spectra are very important because these elements can change the reactivity of surfaces even if the sample is prepared in vacuum. The usual source of this contamination is the air or residual gases in the vacuum. As shown in Fig. 10, the C 1 s spectra can be deconvoluted into three peaks representing three functional groups of C–H, C–O, and C=O at binding energies of 284.80, 286.3, and 288.87 eV, respectively. Table 3 shows that the C–O content (C–OH and C–O–C) decreases from 13.3 to 10% while that of C=O increases from 6.0 to 12.8% due to the arsenic uptake, indicating the oxidation of C–O to C=O on

As loaded magnetite–maghemite sorbent surface. The C 1 s labeled peak is related to the differential charging of a small proportion of the adsorbed As species. This is seen by the small contribution near 42 eV in the As 3d (As(V)) data. There is no indication of charging in the Fe 2p or O 1 s data.

Figure 11 shows O 1 s spectra of the fresh magnetite–maghemite sorbent, arsenite loaded sorbent and arsenate loaded sorbent at pH 5. The peaks at binding energy of 529.4, 531.7, and 531.6 eV can be assigned to Fe–O (lattice oxygen in magnetite–maghemite mixture), As_2O_3 and As_2O_5 (Wagner et al. 1980).

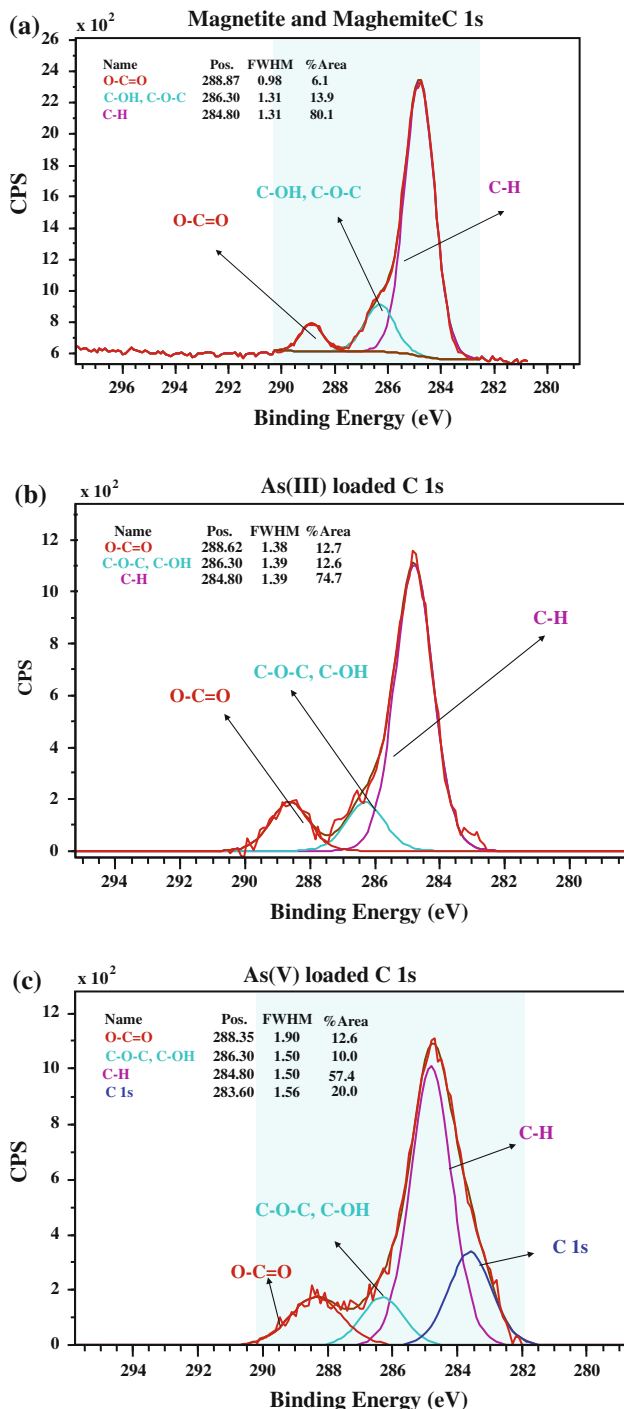


Fig. 10 C 1s XPS spectra of **a** the pure sorbent **b** As(III) loaded **c** As(V) loaded magnetite and maghemite mixture

Compared with the virgin sorbent (Fig. 11a), metal oxide spectrum of the arsenate and arsenite loaded sorbents (Fig. 11b and c) were increased in component peak areas (74.5 and 75.2%, respectively). The spectrum FWHM at 531.08 eV was changed after the adsorption (Fig. 11b, c) indicating As-O on the sorbent surface. Table 1 shows that the metal oxide content increases from 70.7 to 75.2% and O

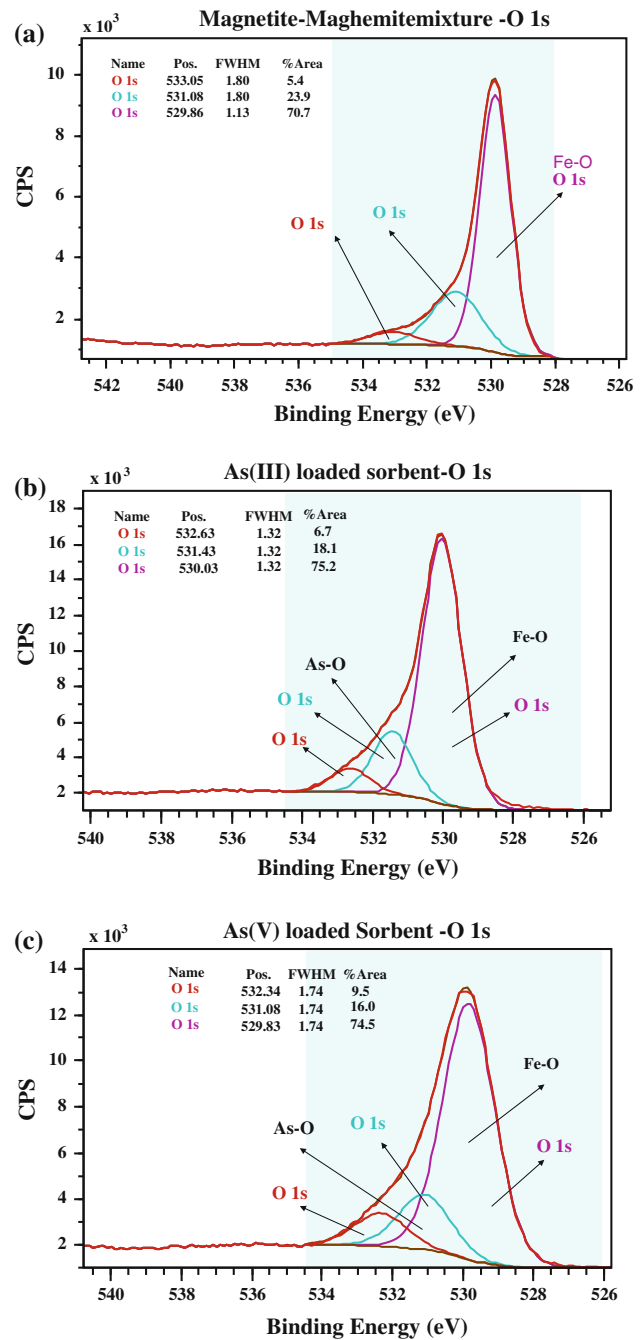


Fig. 11 O 1s spectra of **a** the fresh magnetic-maghemite sorbent and **b** arsenite loaded sorbent **c** arsenate loaded sorbent at pH 5

1 s Hydroxide decreases from 23.9 to 16% indicating the formation of As-O, which is due to the binding of arsenic onto the oxygen atom in the sorbent. Thus, the adsorption mechanism of As(III) and As(V) onto $\text{Fe}_3\text{O}_4-\gamma\text{-Fe}_2\text{O}_3$ surface is suggested to be a physico-chemical reaction as well as electrostatic attraction at pH of 5. The amount of arsenic used in the XPS spectrum analysis was very low (0.1–0.5 atomic percent) compared with the amount of iron detected (24–27 at.%); any iron-arsenic complex contribution to the

Fe 2p spectrum would be obscured by the large magnetite–maghemite signal.

Conclusions

Application of magnetite–maghemite nanoparticles for arsenic removal has great potential in water and wastewater engineering. From this study, it is apparent that the removal of arsenic by magnetite–maghemite nanoparticles depends on pH, contact time, and initial concentration of arsenic. The results show that magnetite–maghemite nanoparticles can adsorb As(III) and As(V) better in an acidic pH range. For 2 mg/L of As(V) and As(III) concentrations, equilibrium was achieved in 3 h at pH 6.5. In groundwater, arsenic adsorption capacity of the magnetite–maghemite nanoparticles at room temperature, calculated from the Langmuir isotherm, was 80 $\mu\text{mol/g}$ and Gibbs free energy (ΔG° , kJ/mol) for arsenic removal was -35 kJ/mol , indicating the spontaneous nature of adsorption on magnetite–maghemite nanoparticles.

X-ray photoelectron spectroscopy (XPS) studies confirmed the presence of arsenic on the surface of magnetite–maghemite nanoparticles. Electrostatic attraction and oxidation–reduction between arsenic and mixed magnetite–maghemite are the postulated mechanism for removal of arsenic from aqueous solutions. To capitalize on this advantage, magnetite–maghemite particles can be used in water treatment and site remediation. Mixed magnetite–maghemite particles may be applied in the design of permeable reactive barriers for groundwater remediation. Permeable reactive barriers containing magnetite–maghemite particles could be employed at a fixed pH for in situ remediation of groundwater contaminated with redox active metals. Proper design and investigation are necessary to find out the applicability of magnetite–maghemite particles for the construction of permeable reactive barriers.

Acknowledgments Funding for the research was provided to by the Natural Sciences and Engineering Research Council of Canada in the form of an Individual Discovery Grant awarded to Dr. E.K. Yanful.

References

- Anderson MA, Ferguson JF, Gavis J (1976) Arsenate adsorption on amorphous aluminium hydroxide. *J Colloid Interface Sci* 54:391
- British Geological Survey (BGS) and Government of the People's Republic of Bangladesh (2001) Arsenic contamination of groundwater in Bangladesh. Technical Report. WC/00/19, vol 1.
- Cornell RM, Schwertmann U (1996) The iron oxides: structure, properties, reactions, occurrence and uses. VCH Publishers, New York, NY (USA). ISBN:3-527-28576-8.
- Demarco MJ, Sengupta AK, Greenleaf JE (2003) Arsenic removal using a polymeric/inorganic hybrid sorbent. *Water Res* 37(1): 164–176
- Dixit S, Hering JG (2003) Comparison of arsenic(V) and arsenic(III) sorption onto iron oxide minerals: Implications for arsenic mobility. *Environ Sci Technol* 37:4182
- Driehaus W, Jekel M (1998) Granular ferric hydroxide—a new adsorbent for the removal of arsenic from natural water. *J Water SRT Aqua* 47:1–6
- Fairley N (1999–2003) CasaXPS Version 2.2.19
- Grosvenor AP, Kobe BA, Biesinger MC, McIntyre NS (2004a) Investigation of multiplet splitting of Fe 2p XPS spectra and bonding in iron compounds. *Surf Interface Anal* 36:1564–1574
- Grosvenor AP, Kobe BA, McIntyre NS (2004b) Examination of the oxidation of iron by oxygen using X-ray photoelectron spectroscopy and QUASES. *Surf Sci* 565:151–162
- Guha S, Chaudhuri M (1990) Removal of As(III) from groundwater by low cost materials. *Asian Environ* 12:42
- Gupta KS, Chen KY (1978) Arsenic removal by adsorption. *J WPCF (Wineries, fresh pack food processors)* 50:493
- Gupta RP, Sen SK (1974) *Phys Rev* 10, 71
- Gupta RP, Sen SK (1975) *Phys Rev* 12, 15
- Harper TR, Kingham NW (1992) Removal of arsenic from wastewater using chemical precipitation methods. *Wat Environ Res* 64:200
- Hossain et al (2005) *Environ Sci Technol* 39:4300
- Hu et al (2004) Removal of Cr(VI) by magnetite nanoparticle. *Water Sci Technol* 50(12):139–146
- Ioannis AK, Anastasios IZ (2002) Removal of arsenic from contaminated water sources by sorption onto iron-oxide-coated polymeric materials. *Water Res* 36:5141–5155
- Karim M (2000) Arsenic in groundwater and health problems in bangladesh. *J Water Res* 34(1):304–310
- Lim SF, Zheng YM, Chen JP (2009) Organic arsenic adsorption onto a magnetic sorbent. *Langmuir* 25(9):4973–4978
- Maeda S, Ohki A, Saikoji S, Naka K (1992) Iron (III) hydroxide-loaded coral lime stone as an adsorbent for arsenic (III) and Arsenic(V). *Sep Sci Technol* 27:681
- Manju GN, Raji C, Anirudhan TS (2000) Treatment of arsenic(III) containing wastewater by adsorption on hydrotalcite. *Ind J Environ Health* 42 (1)
- Mayo et al (2007) The effect of nanocrystalline magnetite size on arsenic removal. *Sci Technol Adv Mater* 8:71–75
- McKay G, Bino MJ, Altamemi AR (1985) The adsorption of various pollutants from aqueous solutions on to activated carbon. *Wat Res* 14:277
- Neff JM (1997) Ecotoxicology of arsenic in the marine environment—review. *Environ Toxicol Chem* 16(5):917–927
- Nesbitt IJ, Pratt AR (1995) Oxidation of arsenopyrite by air and air-saturated, distilled water and implications for mechanism of oxidation. *Geochim Cosmochim Acta* 59(9):1773–1786
- Nordstrom DK, Archer DG (2003) Arsenic thermodynamic data and environmental geochemistry. In: Cai Y, Braids OC, Biogeochemistry of environmentally important trace elements, Oxford University Press, pp 1–25 (Chapter 1)
- Ohe K, Tagai Y, Nakamura S (2005) Adsorption behavior of As(III) and As(V) using magnetite. *J Chem Eng Japan* 38(8):671
- Petrusevski B, Boere J, Shahidullah SM, Sharma SK, Schippers JC (2002) Adsorbent-based point-of-use system for arsenic removal in rural areas. *J Wat SRT-Aqua* 51:135–144
- Prasad G (1994) Arsenic in the environment. Part 1. New York 33.
- Pratt AR, Muir IJ, Nesbitt HW (1994) X-ray photoelectron and auger electron spectroscopic studies of pyrrhotite and mechanism of air oxidation. *Geochim Cosmochim Acta* 58:827–841
- Raven KP, Jain A, Loeppert RH (1998) Arsenite and arsenate adsorption on ferrihydrite: kinetics, equilibrium, and adsorption envelopes. *Environ Sci Technol* 32:344
- Shih M (2005) An overview of arsenic removal by pressure-driven membrane processes. *Desalination* 172(1):85–97

- Shipley HJ, Yean S, Kan AT, Tomson MB (2009) Adsorption of arsenic to magnetite nanoparticles: effect of particle concentration, pH, ionic strength, and temperature. *Environ Toxicol Chem* 28(3):509–515
- Singh DB, Prasad G, Rupainwar DC, Singh VN (1988) As(III) removal from aqueous solution by adsorption. *Wat Air Soil Pollut* 42:373
- Tuutijärvi T, Sillanpää JLM, Chenb G (2009) As(V) adsorption on maghemite nanoparticles. *J Hazard Mater* 166:1415–1420
- Wagner CD, Zatko DA, Raymond RH (1980) Use of the oxygen KLL Auger lines in identification of surface chemical states by electron spectroscopy for chemical analysis. *Anal Chem* 52:1445–1451
- Wang Y, Morin G, Ona-Nguema G, Menguy N, Juillot F, Emmanuel Aubry E, Guyot FO, Calas G, Gordon E, Brown GE (2008) Arsenite sorption at the magnetite–water interface during aqueous precipitation of magnetite: EXAFS evidence for a new arsenite surface complex. *Geochim Cosmochim Acta* 72:2573–2586
- Yean S, Cong L, Yavuz CT, Mayo JT, Yu WW (2005) Effect of magnetite particle size on adsorption and desorption of arsenite and arsenate. *J Mater Res* 20 (12)